Field theoretical interpretation on dynamics of plastic deformation - Portevin-Le Chatelie effect and propagation of shear band

2001 J. Phys.: Condens. Matter 13 6741

(http://iopscience.iop.org/0953-8984/13/31/312)

INSTITUTE OF PHYSICS PUBLISHING JOURNAL OF PHYSICS: CONDENSED MATTER

J. Phys.: Condens. Matter **13** (2001) 6741–6757 PII: S0953-8984(01)22175-4

Field theoretical interpretation on dynamics of plastic deformation—Portevin–Le Chatelie effect and propagation of shear band

S Yoshida[1] **and S Toyooka**[2]

[1] Department of Chemistry and Physics, Southeastern Louisiana University, SLU 10878, Hammond, LA 70402, USA
[2] Department of Environmental Science and Human Engineering, Saitama University, 255 Shimo-okubo, Urawa, Saitama, Japan

Received 13 February 2001, in final form 1 June 2001
Published 19 July 2001
Online at stacks.iop.org/JPhysCM/13/6741

Abstract

The shear band and associated stress relaxation classically known as the Portevin–Le Chatelie effect is considered based on physical mesomechanics, a recent field theory on plastic deformation and fracture. Using the mathematical analogy to the Maxwell's electromagnetic theory, the field theoretical meanings of various properties of plastic deformation are considered. For more intuitive understanding, a simple, two-dimensional spring–mass model is introduced. Along these considerations, interpretations are given to various experimental observations, in which the shear band is detected as an optical interferometric band structure. The results of this investigation are consistent with our previous identification of the optical band structure as a current associated with symmetry.

1. Introduction

In the course of tensile analysis by in-plane displacement sensitive, electronic speckle pattern interferometry (ESPI) [1], we discovered an interesting band structure in fringe patterns [2]. This band structure, called the decorrelation band (DB)[3], was conspicuous because of its sharper edges and more uniform brightness as compared with the surrounding interferometric fringes. The most intriguing feature of the DB was that its motion indicated whether the sample was close to failure and where the failure would occur. It began to appear as soon as the sample yielded and in its early stage it swept across the sample along the tensile axis. After sweeping across the sample several times, it became stationary at a certain location, where the sample eventually failed. Our subsequent studies [3, 4] revealed that when the level of stress concentration is low, the DB is formed intermittently at different locations of the

[3] When we observed this band structure for the first time, it looked brighter in our black and white TV monitor. Therefore, we called it the white band in [2] and all our previous publications. However, since it is caused by decorrelation, and in some cases the brightness is lower than the surrounding bright fringes, it is more appropriate to call it the decorrelation band.

sample, and thereby it appears dynamic, sweeping across the sample along the tensile axis; that when the stress concentration develops to a certain level the DB becomes stationary at the location where the sample eventually fails [3] and that if the sample has a high-level, initial stress concentration the DB can be stationary from the beginning at the location where the sample fails [3]. This feature indicates the possibility of using the DB as an indicator of stress concentration and failure [5].

These observations indicate that the DB is obviously related to stress concentration and to a great extent to the fracture mechanism. From this standpoint, it is likely that the DB represents the shear band, which is associated with the Portevin–Le Chatelie effect [6] and often referred to as the Lüders band[4] [7]. However, the DB and its dynamics cannot be explained by conventional theories of fracture mechanism. We have noticed that most of the previous observations on the DB seem to be explained by physical mesomechanics (PMM) [8–10], a recent gauge theory on plastic deformation (PD) and fracture. According to PMM, PD is a self-consistent wave phenomenon observed in the displacement field as a consequence of symmetry in the associated physics, where the displacement wave carries away the stress energy from the source of stress concentration in the same sense as a Poynting vector carries electromagnetic energy away from the source. The fracture is interpreted as the final stage of PD where the material becomes too dissipative to propagate the displacement wave so that the flow of stress energy stagnates, and consequently, the generation of a discontinuity becomes the only possible channel for the material to relax the stress energy. Thus in PMM the transition from PD to fracture is characterized as the process in which the displacement wave decays. It has been observed that in the transitional stage to fracture, a displacement wave stops travelling, causing a localized strain [11–13]. This mesomechanical picture seems to be consistent with the above mentioned observation that an initially dynamic DB stops sweeping towards failure. More recently, Toyooka *et al* [14] made thorough analyses on DB using the same type of ESPI at a high sampling rate. Consequently, they discovered that the banded region where a DB appears can be resolved into a fine fringe system whose spatial density varies periodically as the DB sweeps across the sample, and that the sweeping speed of the DB decreases monotonically as the sweeping cycle repeats. These observations have provided additional clues to the mesomechanical explanation of the DB.

In this paper we interpret these previous experimental observations on the DB and its dynamics comprehensively using PMM. Note that PMM is universally applicable to any heterogeneous medium, and therefore, the interpretation we will make in this paper is also universal. We will confirm our previous conclusion [15] that the DB can be identified as a current associated with the physical symmetry involved in PD [16]. Based on this identification, the dynamics of the DB will be explained in connection with the propagation of the displacement wave. In section 2, we will present the theoretical basis of PMM, and interpret its meaning along the line of discussion we will develop in later sections. In section 3, we will summarize various observations obtained in a series of tensile experiment in which displacement and DBs are measured by in-plane displacement sensitive ESPI. These experimental observations will be interpreted in section 4.

2. Theoretical basis

This section contains the theoretical basis of PMM. We first show the mathematical formulation based on the principle of gauge transformation and interpret its physical meaning in connection

[4] In some cases the word Lüders band is used to strictly mean a shear band observed in low carbon steel. In this paper, we use the word Lüders band to mean a shear band observed in a given material.

with stress relaxation and fracture. We then introduce a two-dimensional picture that we use to interpret various experimental observations.

2.1. Physical mesomechanics

Details of PMM are found elsewhere [8–10, 16]. In short, PMM is a gauge theory applied to the mechanical field in a heterogeneous medium under PD. PMM describes PD as a transformation of a local bench mark (LBM) in a deformation structural element (DSE). Here the DSE is defined as the unit volume element represented by the same local coordinates. Expressing the LBM in terms of the components of the local coordinates, the transformation can be written as follows.

$$\eta_i^\mu = \beta_i^j \eta_j^\mu \tag{1}$$

where μ represents the external indices, i and j represent the internal indices, η_i^μ is the ith component of the LBM at μ and β is a 3×3 matrix representing a transformation of the GL(3, R) group, the general transformation group of three dimension. GL(3, R) consists of nine independent parameters of real numbers, which corresponds to the nine degrees of freedom, i.e., rotations, translations and change of the LBM components in length. Requesting the Lagrangian to be invariant under this transformation, PMM has introduced a gauge field, and using the least action principle, it has derived a field equation analogous to that of the Maxwell's electromagnetic theory.

After the summation over the group indices, the Maxwell type field equation together with the Bianchi identity leads to the following set of equations [8, 16].

$$\nabla \cdot \vec{V} = J^0 \tag{2}$$

$$\nabla \times \vec{V} = \frac{\partial \vec{\omega}}{\partial t} \tag{3}$$

$$\nabla \times \vec{\omega} = -\frac{1}{c_t^2} \frac{\partial \vec{V}}{\partial t} - \vec{J} \tag{4}$$

$$\nabla \cdot \vec{\omega} = 0. \tag{5}$$

Here $\vec{V} = (u, v, w)$ is the rate of the displacement, $\vec{\omega} = (\omega_x, \omega_y, \omega_z)$ is the angle of rotation of the LBM, c_t is the phase velocity, J^0 and $\vec{J}$ are, respectively, the temporal and spatial components of the four vector corresponding to the charge of symmetry.

$$J^0 = -g^{ij} \eta_i^\alpha \dot{\eta}_j^\alpha / l^2 \tag{6}$$

$$J^\mu = g^{ij} \eta_i^\alpha D_\nu \eta_j^\beta C_{\alpha\beta}^{\mu\nu} / l^2 \tag{7}$$

where g^{ij} is the matrix inverse to the metric tensor of the internal space, D_μ is the covariant derivative, l is the characteristic size of the DSE, and $C_{\alpha\beta}^{\mu\nu}$ is the dimensionless elastic constant of the medium. The right-hand side of equation (6) represents the temporal change of the local bench mark, which corresponds to the stress concentration [17]. The right-hand side of equation (7) represents the spatial variation of the LBM. Note that when the field is purely rotational, i.e., $\vec{\eta}$ is perpendicular to $\vec{D}\eta$, $\vec{J}$ is zero. Since $\vec{J}$ represents dissipation [17], this means that when the field is purely rotational, there is no dissipation.

From equations (3) and (4), the following wave equations can be derived.

$$\nabla^2 \vec{V} - \frac{1}{c_t^2} \frac{\partial^2 \vec{V}}{\partial t^2} = \frac{\partial \vec{J}}{\partial t} + \nabla J^0 \tag{8}$$

$$\nabla^2 \vec{\omega} - \frac{1}{c_t^2} \frac{\partial^2 \vec{\omega}}{\partial t^2} = \nabla \times \vec{J}. \tag{9}$$

These equations indicate that the translational and rotational modes of displacement are transverse waves.

In more material scientific terms, the above-mentioned dynamics can be considered as a process of stress relaxation. When a material yields, it loses the shear stability. Consequently, the deformation becomes spatially non-uniform, and a developed stress concentration is generated. This makes the displacement field vortical, introducing the rotational component in addition to the translational component. Then, these translational and rotational components of displacement interact with each other (called the translational–rotational interaction, TRI) so that the stress is relaxed. In a wave dynamical sense, it can be said that the TRI mechanism carries away the energy flow associated with the stress concentration in the same sense as a Poynting vector carries electromagnetic energy. As the deformation develops, various defects are generated, making the material more dissipative. This makes it less efficient for the TRI to function as a mechanism of stress relaxation, because part of the stress energy is not transferred as a wave, being lost by the dissipating mechanism. Eventually, the material becomes so dissipative that the TRI completely stops functioning, and consequently, the material generates a discontinuity as the alternative mechanism of stress relaxation [18], i.e., it fractures. Based on these considerations, PMM has defined the following pre-fracture criteria [3]: when a material is about to fracture (1) the wavelength of the displacement wave becomes comparable to the sample size (wavelength pre-fracture criterion), (2) the displacement wave becomes a standing wave (standing wave pre-fracture criterion) and (3) a pair of vortices having mutually opposite direction of rotation appear and the sample fails along the boundary of the vortices (vortex pre-fracture criterion).

2.2. Two-dimensional model

Let us consider the above dynamics in a two-dimensional picture so that it can be compared with the measurement by ESPI. Suppose the tensile load is given in the y direction and the sample is in the x–y plane. In this case, equation (4) becomes as follows for x and y directions.

$$\frac{\partial \omega_z}{\partial y} = -\frac{1}{c_t^2}\frac{\partial u}{\partial t} - J_x \tag{10}$$

$$\frac{\partial \omega_z}{\partial x} = \frac{1}{c_t^2}\frac{\partial v}{\partial t} + J_y \tag{11}$$

where u and v are the x and y components of $\vec{V} = (u, v)$. Together with equation (3), these equations represent transverse waves $u(x, y, t)$, $v(x, y, t)$ and $\omega(x, y, t)$. The mechanism that generates these wave characteristics can be pictured by a simple model shown in figure 1, where the dynamics are presented as the motion of DSE. In this model, the forces between neighbouring DSEs are proportional to the deviation from the equilibrium position of the DSEs; i.e., equivalently, the DSEs are connected to each other with a spring. Suppose DSE(x, $y + \Delta y$) rotates anticlockwise for some reason; for example, the DSEs located to the right of DSE(x, $y + \Delta y$) moves upward more than the DSE located on the left does (figure 1). This rotation of DSE(x, $y + \Delta y$) will push DSE(x, y) to the right. Thus DSE(x, y) will move to the right by $X(x, y + \Delta y)$ at the boundary with DSE(x, $y + \Delta y$). On the other boundary, DSE(x, $y - \Delta y$) will resist this movement of DSE(x, y) by trying to push it back to the left. Consequently, the displacement of DSE(x, y) at this boundary, $X(x, y)$, will be different from the other boundary, and this causes DSE(x, y) to rotate. Based on the assumption that the force operating between the DSEs is a spring force, the force that DSE(x, y) receives from DSE(x, $y - \Delta y$) can be written as

$$f(x, y) = -kX(x, y) \tag{12}$$

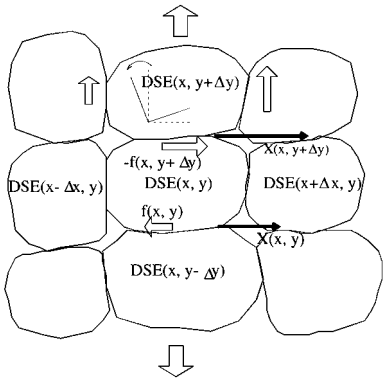

Figure 1. Two-dimensional model of mesomechanical picture of plastic deformation.

where k is the spring constant. Similarly, the force that DSE(x, y+Δy) receives from DSE(x, y) at the other boundary can be written as

$$f(x, y + \Delta y) = -kX(x, y + \Delta y) \tag{13}$$

and the force that DSE(x, y) receives from DSE(x, y+Δy) must be the reaction to $f(x, y+\Delta y)$, i.e., $-f(x, y + \Delta y)$. Therefore the net force that DSE(x, y) receives from these neighbouring DSEs is $-f(x, y + \Delta y) + f(x, y)$, and the equation of motion becomes

$$k[X(x, y + \Delta y) - X(x, y)] = m\frac{\partial u}{\partial t} \tag{14}$$

where m is the mass of the DSE(x, y). In accordance with equation (3), displacement $X(x, y)$ can be related to rotation $\omega_z(x, y)$ as $X(x, y) = -\omega_z(x, y)\Delta y$. Then, expressing $\omega(x, y + \Delta y) - \omega(x, y)$ as $\Delta y \partial\omega/\partial y$, equation (14) becomes

$$k(\Delta y)^2\left(-\frac{\partial \omega_z}{\partial y}\right) = m\frac{\partial u}{\partial t}. \tag{15}$$

For the x direction, the same argument holds, leading to an equation of motion equivalent to equation (15)

$$k(\Delta x)^2\left(\frac{\partial \omega_z}{\partial x}\right) = m\frac{\partial v}{\partial t} \tag{16}$$

where $Y(x, y) = \omega_z(x, y)\Delta x$ was used for the vertical displacement. Putting $\Delta x = \Delta y = \Delta l$, equation (15) and (16) lead to

$$\frac{\partial \omega_z}{\partial y} = -\frac{m}{k(\Delta l)^2}\frac{\partial u}{\partial t} \tag{17}$$

$$\frac{\partial \omega_z}{\partial x} = \frac{m}{k(\Delta l)^2}\frac{\partial v}{\partial t}. \tag{18}$$

These equations reduce to equations (10) and (11) with $J_x = J_y = 0$ and interpreting $m/\{k(\Delta l)^2\} = 1/c_t^2$ (i.e., $\sqrt{m/k} = \tau/2\pi$, $1/\Delta l = 2\pi/\lambda$ where τ is the period and λ is the wavelength of the displacement wave). Indeed, by partially differentiating equation (17) with respect to y and partially differentiating equation (18) with respect to x, and adding them together we obtain the z component of equation (9) with $\vec{J} = 0$. It should be noted that with the condition $\vec{J} = J^0 = 0$, the wave equations (8) and (9) represent non-decaying waves. From this standpoint, the first terms of equations (10) and (11)

represent the synergetic interaction between the translational and rotational mode causing the wave characteristics in the displacement, and the second terms represent the dissipation. Note that in this formulation, the force exerted from the horizontally neighbouring DSEs $\Delta f = f(x + \Delta x, y) - f(x, y) = -k\partial X/\partial x \Delta x$ can be interpreted as part of J_x, because it does not contribute to the wave propagation. A little consideration [17] reveals that these forces are associated with the motion of stress concentration, which corresponds to an electric charge in the analogy to the Maxwell electromagnetic theory (called the EM analogy, hereafter). It is interesting to note that in the EM analogy, the first term corresponds to the displacement current and the second term corresponds to the conduction current, which represents the ohmic loss.

3. Summary of experimental observations

In this section, we summarize various experimental observations on the DB. In the next section, these observations will be discussed based on the mesomechanical interpretation of the DB. Note that all the experiments discussed here are tensile experiments with a constant elongation rate, where displacement is measured by in-plane displacement sensitive ESPI.

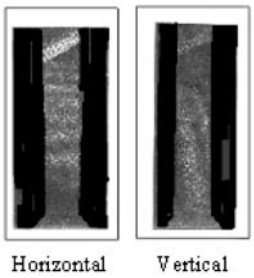

Figure 2. Typical DB observed in HSF and VSF. Also see figure 4 (HSF) and figure 6 (VFS), which show clearer fringe patterns above the DB.

3.1. Observation 1: fringes around DB represent bodily rotation

Figure 2 shows typical DBs observed in fringe patterns representing the horizontal and vertical displacements (called the horizontally sensitive fringe pattern, HSF, and the vertically sensitive fringe pattern, VSF, respectively). Note that the DBs appear at the same location in the HSF and VSF, which indicates that the DBs observed in HSF and VFS represent the same phenomenon. Note that the fringes above and below the DB in the HSF are roughly equidistant and horizontal (see figure 4 for fringes above the DB in HSF), while the fringes above and below the DB in the VSF are roughly equidistant and vertical (see figure 6 for fringes above the DB in VSF). These patterns of fringes indicate bodily rotations of the sample [2, 19] above and below the DB[5].

[5] When a sample rotates as a rigid body by a small angle α, the horizontal and vertical displacement at (x, y) can be written as $\Delta x = -\alpha y$ and $\Delta y = \alpha x$, respectively. Thus the horizontal displacement depends only on the vertical coordinates, whereas the vertical displacement depends only on the horizontal coordinates. Therefore, the fringes in the HSF, which are contour lines of equi-displacement in the horizontal direction, appear to be equidistant from one another and parallel to the x axis. For the same reason, the fringes in the VSF appear to be equidistant from one another and parallel to the y axis.

3.2. Observation 2: DB moves when stress concentration is at a low level

Experimental studies on the DB under various stress conditions [3] have revealed that the appearance of the DB strongly depends on the level of stress concentration. In the case where the sample does not have an initial stress concentration, the DB typically begins to appear as soon as the sample yields. In an early stage, the DB usually runs approximately in the direction of the maximum shear stress, i.e., about 45° to the tensile axis. In this stage, sometimes more than one DB appear at different locations of the sample simultaneously. The DB of this stage normally sweeps across the sample along the tensile axis, and therefore appears to be dynamic. When the stress reaches a certain level, the DB becomes stationary at the location where the sample eventually fails. In this stage, the DB is not necessarily at 45° to the tensile axis, but runs along the line of forthcoming failure. Figure 3 shows a typical time-historical trace of the DB observed in this type of sample. In the case where the sample has an initial stress concentration such as a welded joint, the DB appears to be stationary from the beginning at the location where the sample eventually fails [3, 5]. If the initial stress concentration is intense, the DB sometimes begins to appear at the stage where the stress–strain curve is still in the elastic region [3]. In any case, the sample always fails at the location where the DB becomes stationary, and the failure occurs along the DB.

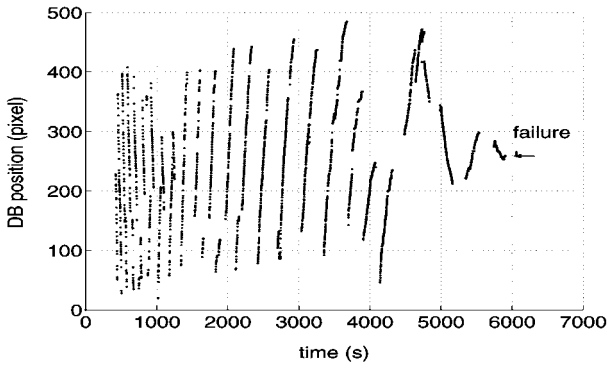

Figure 3. Time historical trace of DB. The vertical axis indicates the pixel number of the CCD camera that takes ESPI images. The sample failed where the DB finally became stationary.

The way the DB drifts depends on the type of material [4]. In the case of aluminum alloys, the DB sweeps across the length of the sample several times before it becomes stationary [3, 4]. In some cases, the DB changes the direction of its sweep [4]. On the other hand, it has been observed that in the case of a steel, the DB sweeps only once in one direction on the yielding plateau of the stress curve [4, 20].

3.3. Observation 3: DB observed at the boundary of vortices

In [21], we observed that a DB appears at the boundary of a pair of vortices in the field of the secondary time-derivative of displacement. Figure 4 illustrates the situation. Here the field of the secondary time-derivative of displacement is evaluated by subtracting the rate of displacement measured in the preceding time step from that measured in the current time step. The DB began to appear immediately after these vortices appeared. Note that the vortices have mutually opposite directions of rotation and that the secondary time-derivative of displacement is proportional to the force. These indicate that the DB appears along the region where an intense bend-torsion moment operates. This particular DB was stationary from the beginning,

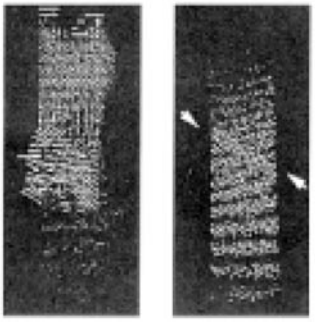

Figure 4. The vortical field of the secondary time-derivative of displacement (left) and the DB that appears in an HSF immediately after the vortex is observed (right). Note that the DB appears along the boundary of the vortices.

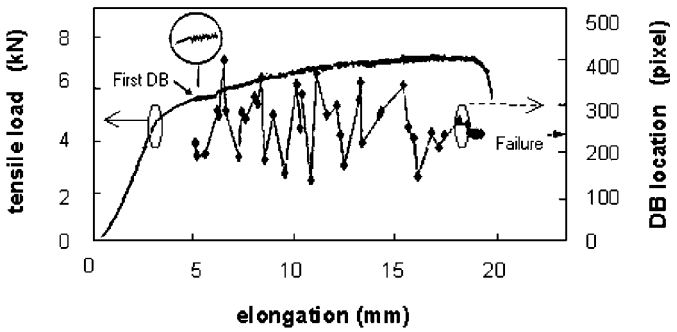

Figure 5. DB and stress drop.

and the sample failed along this location. This observation is consistent with the vortex pre-fracture criterion mentioned in section 2.1.

3.4. Observation 4: DB is accompanied by a stress drop

We have noticed that the appearance of a DB coincides with a stress drop [3, 21]. Figure 5 illustrates the situation where the stress drops as a dynamic DB appears at different locations, making the stress–strain curve zigzag (the phenomenon known as the Portevin–Le Chatelie effect or a serrated loading curve [6]). Zhang *et al* [22] and Makarov and Romanova [23] also observed the same phenomenon in their experimental and theoretical investigation, respectively.

3.5. Observation 5: finer fringes are observed in DB

Toyooka *et al* [14] have employed a high sampling rate to increase the temporal resolution of ESPI and discovered that the banded region where a DB appears can be resolved into a fine fringe structure. Figure 6 shows fine fringes such as they observed in the vertical displacement (in the tensile direction) with a sampling rate of 30 frames s^{-1}. Each fringe pattern represents deformation occurring in 1/6 s^{-1} (five frames) at a tensile speed of 3.9 μm s^{-1}, while one fringe spacing corresponds to displacement of 0.35 μm. The number shown under each pattern is the frame number, indicating the elapsed time from a reference frame. The rightmost pattern

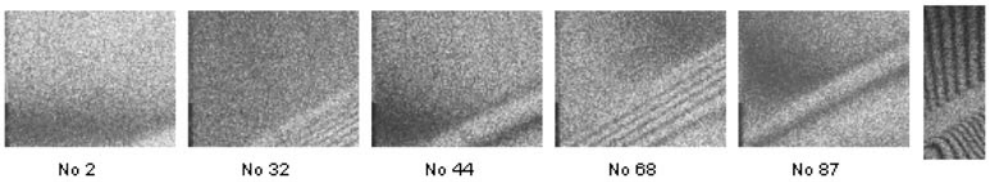

Figure 6. Fine fringe structure observed in the banded region where a dynamic DB appears. The rightmost photograph shows the fringe system of a whole view of the sample observed with a second camera. All fringe patterns are VSFs. After Toyooka *et al* [14].

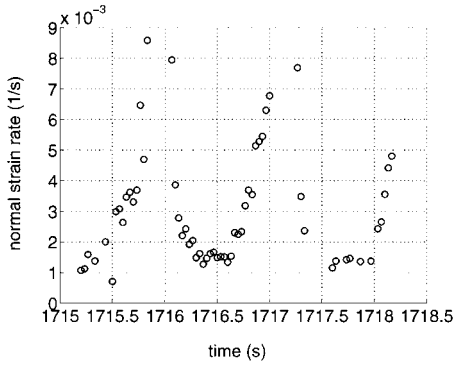

Figure 7. Strain pulsation. Note that in [14] the authors define the x axis as the vertical axis but in this paper we define the y axis as the vertical axis.

shows a fringe system that they observed in the same experiment with a second camera viewing a whole field of the sample at a lower sampling rate (40 frames min^{-1}). This pattern (called the whole-field pattern) represents deformation occurring in 1.5 s. Note that the fine fringe system is always formed at the location where a DB appears and it moves together with the DB. The entire fine fringe structure, having two to six fringes depending on the frame, corresponds to a single DB seen in the whole-field pattern. Note that six fringes correspond to a total elongation of $0.35\ \mu\mathrm{m} \times 6 = 2.1\ \mu\mathrm{m}$, if all the fringes represent elongation, and that this value is greater than the motion of the tensile machine's grip calculated as $3.9\ \mu\mathrm{m\ s}^{-1} \times 1/6\ \mathrm{s}^{-1} = 0.65\ \mu\mathrm{m}$. This indicates that when the fine fringe structure shows six fringes, they represent, at least partially, contraction of the material.

3.6. Observation 6: strain in DB varies periodically

In [14], the authors note that the density of the fine fringes changes periodically, and call the effect the strain pulsation. Figure 6 illustrates the situation where the fringe density alternates between the dense and coarse state. When the fringe density is in the coarse state, the total number of fringes is typically two. Since one fringe spacing corresponds to a displacement of 0.35 μm, this means that the total elongation in the vicinity of a DB is about $0.35\ \mu\mathrm{m} \times 2 = 0.7\ \mu\mathrm{m}$, which is roughly equal to the distance that the grip of the tensile machine travels ($3.9\ \mu\mathrm{m\ s}^{-1} \times 1/6\ \mathrm{s}^{-1} = 0.65\ \mu\mathrm{m}$). This indicates that the coarse state corresponds to the situation where the elongation caused by the tensile machine is concentrated in the region of the DB.

Figure 7 shows the strain pulsation effect observed in figure 6 in terms of the temporal variation of the fringe density per unit time [14]. Since this fringe system represents the

vertical displacement, figure 7 effectively represents the rate of the normal strain in the vertical direction, where the peak of the normal strain rate corresponds to the dense fringe state in figure 6 while the valley corresponds to the coarse fringe state. The strain rate shows clear periodicity with a period of 1 s.

3.7. Observation 7: DB drift velocity is similar to the phase velocity of a u-wave observed in a similar material

We observed dynamic DBs in an aluminum alloy a number of times [2, 3, 13], and have found that those DBs show similar drift velocities to each other. In [13] we observed displacement waves in the displacement component perpendicular to the tensile axis (called the u-wave). We observed that the u-wave initially travelled along the tensile axis and became stationary before the sample failed, in consistence with the standing wave pre-fracture criterion. We have noticed that this phase velocity that the u-wave shows in its initial stage is quite similar to the above-mentioned drift velocities of the dynamic DBs[6].

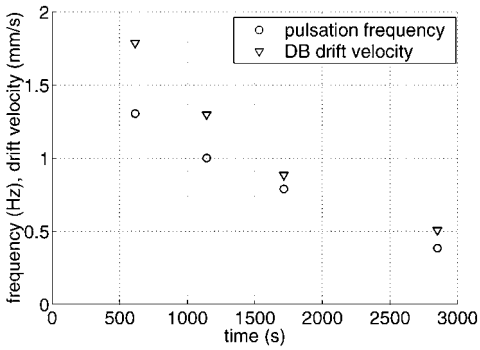

Figure 8. Temporal variation of pulsation frequency and DB drift velocity as deformation progresses. After Toyooka *et al* [14].

3.8. Observation 8: DB drift velocity decreases and becomes zero at failure

Figure 3 indicates that as the DB repeats the sweep across the length of the sample, its drift velocity decreases. Figure 8 shows this effect explicitly, as observed by Toyooka *et al* [14]. A similar decrease in the drift velocity of DB has been observed in other measurements [2, 3]. Note that the drift velocity always becomes completely zero when the sample fails, as seen in figures 3 and 5. Also shown in figure 8 is the observation by Toyooka *et al* [14] that as the drift velocity of the DB decreases the frequency of the strain pulsation decreases.

[6] In those series of experiments where we observed the displacement wave, the DB began to appear after the displacement wave became a standing wave and it was stationary from the beginning. On the other hand, in the other series of experiments where we observed dynamic DBs the displacement waves were too complicated to extract the phase velocities. Therefore, it was impossible to compare the phase velocity of the displacement wave and the drift velocity of the DB directly in the same experiment. However, as discussed in [13], the phase velocity is likely to be a constant for a given material with a given sample length. From this standpoint we say that this observation implies that the drift velocity of DB is similar to the phase velocity of the displacement wave.

4. Interpretation of the experimental observations

From the mesomechanical viewpoint, the DB can be interpreted as manifestation of current J [15]. Let us consider the DB from the viewpoint of more conventional mechanics and discuss the meaning of current J, accordingly. The observations described under subsection 3.2 in the preceding section (hereafter we abbreviate these subsections as obs 2, etc) are quite similar to the properties of a Lüders band [7]. Classically, it is explained that a Lüders band is formed when a number of dislocations move one after another in a chain reaction known as the cataclysmic release of dislocations [24]. Because a movement of dislocation causes a slip, the resemblance to the Lüders band indicates that the formation of the DB is associated with a slip. Thus the following scenario can be naturally pictured. When the stress reaches a certain level, a slip occurs at the boundary of two adjacent DSEs, as one of them (the primary DSE) pushes the other (the secondary DSE) by the type of motion described in the above-introduced two-dimensional picture. Because of this slip, the motion of the primary DSE is not completely transferred to the secondary DSE; in other words, the kinetic energy associated with the motion of the primary DSE is partially dissipated. In equation (10), the first term on the right-hand side represents the transfer of the motion of the primary DSE to the secondary DSE as a wave, while the second term (the J current term) represents dissipation. Thus the DB can be interpreted as this type of slip initiated at some point on the boundary of neighbouring DSEs and flows across the sample width as current J[7]. It is likely that on the right-hand side of equation (10) this process corresponds to an increase in the second term and a decrease in the first term. Since the first term is proportional to the acceleration, the decrease in this term basically represents a decrease in force [13, 18]. In the above picture, this corresponds to the situation where because of the slip the resisting force by the secondary DSE reduces. This picture is consistent with the observation that a stress drop accompanies the appearance of DB (obs 4). It is interesting to note that in the EM analogy this is equivalent to the situation where as a medium under an electric potential becomes more conductive, the displacement current (corresponding to our first term) decreases and the conduction current (corresponding to our second term) increases [18]. From the gauge theoretical viewpoint, the conduction current and current J are commonly interpreted as the current of a charge that is invariant under the transformation. Also note that part of the displacement resulting from such a slip is unrecoverable in the next phase of the displacement wave in which the DSEs move in the opposite directions. This corresponds to the phenomenon known as the yield elongation, an elongation that takes place around the yield point with no stress increase and during which a Lüders band propagates along the sample. Because the elongation takes place without an increase in stress, it remains after the stress is removed, i.e., the elongation is unrecoverable.

Along the above scenario, let us consider the other observations on DB. From the observation that a DB appears at the boundary of vortices where an intense bend–torsion moment operates (obs 3), the situation of the sample when a DB is about to appear can be considered to be as shown in figure 9. Because of non-uniformity in the vertical elongation, the type of bend–torsion moment described in obs 3 is generated around a weak region where deformation is being concentrated. This creates the situation where the part of the sample above this deformation-concentrated region rotates in one direction, say clockwise for example, pulling the other part of the sample so that it rotates in the other direction (i.e., anticlockwise). When this bend–torsion moment reaches a certain level, it becomes impossible for the lower part to follow the motion of the upper part, and slip occurs over the horizontal width of the

[7] This picture is consistent with the interpretation made by Panin *et al* [25] that a DSE rotate as a whole by means of current J. Note that current J flows along the boundary of DBs, and this flow is different from the drift of the DB, which represents the fact that the DB appears at different locations at different times.

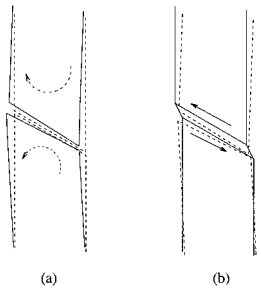

Figure 9. Schematic view of the formation of a DB. An intense bend–torsion moment is generated so that the upper and lower parts of the sample receive rotational forces in mutually opposite directions (a). When the stress reaches the threshold level, a slip occurs at the boundary of the vortices and a DB runs.

sample. Consequently, the stress drops and the lower part bounces back clockwise as the upper part keeps moving in the same direction with effectively no resistance from the lower part. This slipping motion is observed as a DB being accompanied by bodily rotations of the sample above and below the DB (obs 1).

In the spring–mass model, this process is equivalent to the following situation. Imagine that we are dragging a mass using a spring and that the mass is connected to a second mass behind it with a second spring. Here, the first mass corresponds to the primary DSE and the second mass corresponds to the secondary DSE. As we go forward the resisting force from the first spring increases. When the resisting force reaches a certain value, the first spring behind us can no longer tolerate the force and partially breaks (i.e., it loses the function as a spring with the original spring constant while keeping the capability of providing a recovery force). Then all of sudden the force from the first spring decreases and we will be thrown forward. At the same time, the first mass we have been dragging will be pulled backward by the second spring, and consequently, the force to the second spring is reduced. This corresponds to the moment when a slip occurs and the stress drops. In the material scientific picture, this is when a dislocation is released. A moment later, the DSEs are rearranged and a new equilibrium is established with new equilibrium positions of the DSEs. Accordingly, a new spring with a slightly lower spring constant (see below) is created, and the stress increase resumes. The displacement corresponding to the difference between the original and new equilibrium positions is not recoverable.

This bouncing-back motion of the lower part continues until the new equilibrium is established, consuming the displacement cumulatively gained in the past at the boundary with the upper part. While this happens, the upper part keeps moving in the opposite direction being driven by the tensile machine. The pulsation effect observed in figures 6 and 7 is the indication of this bouncing-back phenomenon taking place in the displacement component parallel to the tensile axis. The coarse-fringe state corresponds to the stage in which the deformation is being concentrated and the dense-fringe state corresponds to the stage in which the bouncing-back motion is taking place. This explains why the number of the coarse fringes corresponds to a displacement similar to the motion of the grip while the number of dense fringes corresponds to a displacement greater than the motion of the grip (obs 5). When the slip completes, the stress restarts to increase causing a concentrated deformation and the same process repeats. This explains the periodical change of the strain around the DB (obs 6). From this viewpoint, the period in normal strain rate observed in figure 7 can be interpreted as representing the stress recovery time.

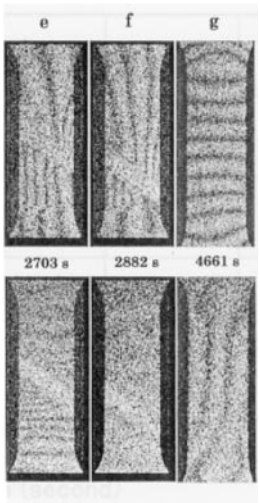

Figure 10. Fringe patterns observed with a DB (e and f) and without a DB (g). The upper patterns are VSF and the lower patterns are HSF. The fringe pattern accompanied by a DB represents bodily rotations above and below the DB, while the fringe pattern not accompanied by a DB represents fairly uniform normal strain. Numbers indicate the elapsed time from the moment when the sample started to be loaded. After Suprapedi [26].

It is interesting to analyse the fringe patterns in connection with the type of strain that the sample is undergoing. Figure 10 shows whole-field fringe patterns (VHFs in the upper row and HSFs in the lower row) observed at an early stage of PD (past the yield point by about 10% of the total elongation that the sample undergoes before it fails). In this stage, the DB is formed intermittently on fringe patterns at different locations of the sample, thereby it appears to be sweeping along the tensile axis at a constant drift velocity. In terms of the explanation made in the preceding paragraph, this is the stage in which the formation of a slip and the stress recovery repeat alternatively. Figure 10 indicates that when a DB is formed (e and f) the pair of VSF and HSF represents bodily rotations of the sample above and below the DB, whereas when a DB is not formed (g) both VSF and HSF indicate fairly uniform normal strain spread over the whole sample. Here the fringe pattern representing bodily rotation can be characterized by equidistant, vertically parallel fringes in the VSF, and equidistant, horizontally parallel fringes in the HSF [19]. These observations can be interpreted as follows: during the period in which a DB is being formed the deformation is concentrated in the banded region so that the upper and lower parts of sample undergo bodily rotations as discussed above. Once the DB is formed, the stress is relaxed accordingly. Consequently, the material momentarily goes back to a stress situation similar to the elastic regime. This makes the sample undergoes relatively uniform normal strain as typically observed in elastic deformation, and this situation is represented by the fringe pattern shown in figure 10(g).

Also of interest is to note in figure 6 that the fine fringe system observed within the banded region of the DB shows normal strain ($\partial v/\partial y$) while the whole-field fringe pattern (the rightmost pattern) taken at the same time represents the bodily rotation of sample above and below the DB. Note that this normal strain in the fine fringe system is concentrated in the banded region, being contrastive to the above-mentioned uniform normal strain typically observed in the elastic regime. Obviously, these two types of normal strain are different from each other in their mechanisms of formation. The former is due to localized deformation concentrated

in the banded region where a DB is being formed, whereas the latter is associated with rather uniform deformation occurring over the whole sample. In the basic equations (2)–(5), the normal strain terms appear only in equation (2), representing charge J^0. Thus this observation can be interpreted as follows: when a DB is about to appear, deformation is concentrated around the region where the DB is being formed, and this deformation contains concentrated normal strain that corresponds to charge J^0. When the DB is formed, the charge flows as current J and, consequently, the stress is relaxed. This interpretation is consistent with the previous interpretation [15] that the DB is identified as current J, because J is the flow of J^0. Note that in the EM analogy, J^0 corresponds to an electric charge. When an electric charge flows in a conductive medium, it reduces the electrical potential applied across the medium and causes energy dissipation known as the ohmic loss. In such a picture, the stress relaxation by means of current J corresponds to the reduction in the electric potential and the associated dissipation corresponds to the ohmic loss[8].

Now we consider the drift of the DB. Suppose a DB is formed at a certain location of the sample. In accordance with the above interpretation, the formation of the DB can be explained by the following dynamics. When the displacement grows to a certain level at some location, the stress reaches the threshold value to cause a slip. As the slip occurs, the displacement reduces at all the points above and below this location and a new equilibrium position is established. Remember that in this model the displacement represents the distance from the equilibrium position (see the paragraph following equation (11)). It will be helpful to consider the situation using figure 1 which represents the horizontal component of the dynamics. Imagine that a slip occurs at the boundary between DSE(x, $y + \Delta y$) and DSE(x, y). This will lower the force $f(x, y)$ at the other boundary of DSE(x, y), reducing the displacement $X(x, y)$ there. Similarly, on the other boundary of DSE(x, $y + \Delta y$) the displacement $X(x, y + 2\Delta y)$ will reduce. (The vertical displacement is reduced by the same mechanism and is represented by the pulsation effect (obs 6).) After this reduction takes place, the displacement increases again because the sample is still under the external load; then after a while, the stress reaches the threshold value again to cause another slip. While this happens, the displacement will travel as a transverse wave, where the u-wave represents its horizontal component propagating in the vertical direction. Therefore, during the period in which the stress recovers from the reduced level associated with the last slip to the threshold level causing the next slip, the u-wave will travel in the vertical direction for a distance equal to its phase velocity (i.e., the vertical component of the phase velocity of the total displacement wave) times the recovery time. This distance is observed as the vertical distance of the two consecutive DBs. This explains why the drift velocity of the DB is similar to the phase velocity of the u-wave (obs 7).

By this mechanism, the DB drifts towards one end of the sample along with the displacement wave. At this point, the displacement wave is either reflected or transmitted through depending on the boundary condition. While the reflection and transmission of a displacement wave are subjects of future investigation, it will be worth making a few comments. In general, a wave is reflected at a boundary where the material constant varies and thereby the propagation constant changes. In the EM analogy, as an example, an electromagnetic wave is reflected at a boundary where the real part of the electric susceptibility (i.e., the index of refraction) varies. In the present case, the displacement wave will be reflected when it travels through a boundary where the spring constant varies. (Note that a change in the spring constant changes the propagation constant through $\sqrt{m/k} = \tau/2\pi$. See the paragraph under equation (18).) In figure 3 the DB initially travels from the top to the bottom. At 1000 s^{-1},

[8] From this viewpoint, the force associated with the normal strain corresponds to a Coulomb force, which is a longitudinal effect.

it changes direction near the bottom of the sample. Then it keeps sweeping upward until 4800 s^{-1} when it changes direction again near the top of the sample. After that it changes direction a couple of times near the centre of the sample where it fails at 6000 s^{-1}. A possible interpretation of this phenomenon is as follows. Based on the argument made above, as the DB is repetitively formed the spring constant of the sample decreases. It is likely that this decrease in spring constant is greater in the main part of the sample than the wider part at both ends where the sample is gripped by the tensile machine. Therefore, as the deformation progresses the spring constant in the main part becomes smaller relative to the wider part, and at some point of time, the difference in the spring constant between the two parts becomes so great that the displacement wave is mostly reflected near the shoulder of the sample (i.e., the boundary between the main part and the wider part). The first two reflections near the two ends of the sample observed in figure 3 (at 1000 s^{-1} and 4800 s^{-1}, respectively) can be explained by this mechanism. When the deformation develops to the final stage where the strain is concentrated at a certain location of the sample, the spring constant of that region will become considerably lower than the other part of the sample. Thus the reflection will take place at the boundary of this strain-concentrated region. The final couple of reflections observed in figure 3 can be explained by this effect. As the deformation further progresses from this stage, the strain-concentrated region will be further localized. This explains why figure 3 converges to the location where the sample eventually fails. Note that the reflected wave interferes with the wave travelling in the original direction, and consequently, a standing wave can be generated. This explains why the drift velocity of the DB becomes completely zero toward the failure (obs 8).

When a DB sweeps the sample, a slip occurs as the DB is formed at a new location. As discussed above, a slip is equivalent to partial breakage of the spring. Thus, as the DB repeats the sweep, the spring constant decreases. When the spring constant decreases, three things happen. First, the rate of the work hardening decreases. Basically, the spring constant represents the force per unit elongation. Therefore if the tensile load is given at a constant tensile speed as is the case of all the experiment shown in the previous section, the decrease in the spring constant results in a decrease in the rate of increase in force (i.e. the rate of stress increase on the stress–strain curve). Consequently, the stress recovery time increases every time after a slip occurs (i.e., it takes longer to gain a certain stress increase). This explains why the pulsation frequency (i.e., the inverse of the stress recovery time) decreases as the deformation develops (obs 8). Second, the phase velocity of the displacement wave decreases ($c_t = \sqrt{k/m}\Delta l$). This explains why the drift velocity of DB decreases as the deformation develops toward failure (obs 8). Third, the period becomes longer ($\tau = 2\pi\sqrt{m/k}$ [13]). From this standpoint, the failure can be interpreted as the situation where the period of the oscillatory motion of the displacement becomes infinitely long.

5. Summary

We have considered the DB and its dynamics from the viewpoint of PMM. It has been found that the DB is manifestation of a slip of DSE, corresponding to the classical phenomenon known as the Portevin–Le Chatelie effect or the propagation of the Lüders band. In the mesomechanical picture, a slip of DSE is a dissipation process. Therefore, if such a slip occurs, the TRI mechanism becomes less efficient, and the displacement wave as a carrier of the stress energy decays. Consequently, current J flows as the alternative mechanism of stress relaxation. This observation is consistent with the previous interpretation of the DB as current J [15].

We have introduced a simple spring–mass model to intuitively explain the dynamics responsible for the dissipative wave characteristics of the displacement field. In this model, the

stress drop caused by a slip is interpreted as a partial breakage of the spring, which is followed by the creation of a new spring with a lower spring constant. In the mesomechanical picture, this corresponds to the establishment of a new equilibrium in the DSE position and recovery of stress increase. The drift of the DB is interpreted as the travel of the displacement wave during the period of stress recovery. As the DB repeats the sweep along the sample, the spring constant decreases monotonically. Based on this interpretation, the experimental observation that the drift velocity of DB is similar to the phase velocity of the displacement wave can be explained. The observation that towards failure the drift velocity of DB decreases while the period of the oscillatory motion of displacement increases can also be explained. Since the displacement associated with the slip is not stored as the potential energy, it is unrecoverable and remains as permanent strain.

The DB and its involvement in the fracture mechanism is well explained by the EM analogy. The fact that the fine fringe system observed in the DB shows concentrated normal strain component indicates that the associated stress concentration corresponds to an electric charge, being consistent with the above-mentioned interpretation of DB as current J. The transition from PD to fracture can be interpreted as being equivalent to an increase in the imaginary part of the dielectric constant of the medium that an EM wave is propagating through. In this way, the medium becomes more conductive, causing the EM wave to decay, and at the same time, the ohmic loss caused by the conduction current to increase. As previously discussed, this picture indicates the similarity between the electrical breakdown of a gas and fracture of a solid-state material [18].

Acknowledgments

We are grateful to Dr Malik Rakhmanov of University of Florida for valuable discussions and advice.

References

[1] Lokberg O J 1993 Recent development in video speckle interferometry *Speckle Metrology (Optical Engineering Vol 38)* ed R S Shiroi (New York: Dekker) pp 157–94

[2] Yoshida S *et al* 1996 Direct observation of developed plastic deformation and its application to nondestructive testing *Japan. J. Appl. Phys.* **35** L854–7

[3] Yoshida S *et al* 1998 Optical interferometric technique for deformation analysis *Opt. Express* **2** 516–30

[4] Toyooka S, Suprapedi and Zhang Q C 1998 Speckle interferometry to investigate degradation process of stressed solid materials *Proc. SPIE 3407, Int. Conf. on Applied Optical Metrology* (Bellingham, WA: SPIE) pp 400–5

[5] Yoshida S *et al* 1997 New optical interferometric technique for stress analysis *Proc. 3rd Int. Conf. on Modern Practice in Stress and Vibration Analysis (Dublin, 1997)* ed M D Gilchrist, pp 361–3

[6] Mertens F, Franklin S V and Marder M 1997 Dynamics of plastic deformation front in an aluminum alloy *Phys. Rev. Lett.* **78** 4502–5

[7] Lüders W 1860 Ueber die Aeu erung der Elasticität an stahlartigen Eisenstäben und Stahlstäben, und über eine beim Biegen solcher Stäbe beobachtete Molecularbewegung *Dinglers Polytech. J.* **155** 18–22 (in German)

[8] Panin V E (ed) 1998 *Physical Mesomechanics of Heterogeneous Media and Computer-Aided Design of Materials* vol 1 (Cambridge: Cambridge International Science)

[9] Panin V E, Grinyaev Yu V, Egorshkin V E, Buchbinder I L and Kul'kov S N 1987 Spectrum of excited state and the rotational field in a deformed crystal *Izv. VUZ Fiz.* **1** 34–51

[10] Panin V E 1995 Physical mesomechanics of plastic deformation and experimental results obtained by optical methods *Oyobuturi* **64** 889–94

[11] Zuev L B 1992 private communication

[12] Yoshida S, Hida Y, Panin V E and Zuev L B 1994 Application of the wave theory of plastic deformation to a novel scheme of non-destructive analysis of mechanical behavior of solid-state object *Strength of Materials 1994* ed H Oikawa *et al*, pp 295–8

[13] Yoshida S *et al* 1999 Observation of plastic deformation wave in a tensile-loaded aluminum-alloy *Phys. Lett.* A **251** 54–60
[14] Satoru Toyooka, Rini Widiastuti, Zhang Qingchuan and Hiroshi Kato 2001 Dynamic observation of localized strain pulsation generated in the plastic deformation process by electronic speckle pattern interferometry *Japan. J. Appl. Phys.* **40** 310–13
[15] Yoshida S 1999 Optical interferometric study on deformation and fracture based on physical mesomechanics *J. Phys. Mesomech.* **2** 5–12
[16] Egorshkin V E 1990 The gauge dynamic theory of defects in unhomogeneous deformed media with structure. The behavior of boundary *Phis. Izv.* **33** 51–68 (in Russian)
[17] Yoshida S 2001 Mesomechanics as a wave theory analogous to Maxwell electromagnetic theory *CADAMT 2001 (Tomsk, 2001)*
[18] Yoshida S 2000 Consideration on fracture of solid-state materials *Phys. Lett.* A **270** 320–5
[19] Yoshida S, Suprapedi, Widiastuti R, Astuti E T and Kusnowo A 1995 Phase evaluation for electronic speckle-pattern interferometry deformation analyses *Opt. Lett.* **20** 755–7
[20] Toyooka S, Suprapedi, Hauta-Kasari M and Zhang Q C 1998 Dynamic observation of Lüders band propagation by ESPI *3rd Japan–Central Europe Joint Workshop on Modeling and Simulation of Non-Linear Engineering System and Related Phenomena (Bratislava 1998)*
[21] Yoshida S *et al* 1997 Optical interferometry applied to analyze deformation and fracture of aluminum alloys *Theor. Appl. Fract. Mech.* **27** 85
[22] Zhang Q C, Toyooka S, Meng Z B and Suprapedi 1999 Investigation of slip-band propagation in aluminum alloy with dynamic speckle interferometry *Proc. SPIE* **3585** 389–98
[23] Makarov P V and Romanova V A 2000 Mesoscale plastic flow generation and development for polycrystals *Theor. Appl. Fract. Mech.* **33** 1–7
[24] Holden A N 1952 Dislocation collision and the yield point of iron *Trans. AIME* **194** 182–8
[25] Panin V E *et al* 1991 private communication
[26] Suprapedi 1999 Study of speckle pattern interferometry for spatio-temporal analysis of deformation process of stressed materials *Doctoral Thesis* Saitama University, p 73